OPEN

A Role for Peroxisome Proliferator-Activated Receptor Gamma Agonists in Counteracting the Degeneration of Cardiovascular Grafts

Anna Kathrin Assmann, MD, Daniel Goschmer, Yukiharu Sugimura, MD, Agunda Chekhoeva, Mareike Barth, MD, Alexander Assmann, MD, PhD, Artur Lichtenberg, MD, PhD, and Payam Akhyari, MD, PhD

Abstract: Aortic valve replacement for severe stenosis is a standard procedure in cardiovascular medicine. However, the use of biological prostheses has limitations especially in young patients because of calcifying degeneration, resulting in implant failure. Pioglitazone, a peroxisome proliferator-activated receptor gamma (PPAR-gamma) agonist, was shown to decrease the degeneration of native aortic valves. In this study, we aim to examine the impact of pioglitazone on inflammation and calcification of aortic valve conduits (AoC) in a rat model. Cryopreserved AoC (n = 40) were infrarenally implanted into Wistar rats treated with pioglitazone (75 mg/kg chow; n = 20, PIO) or untreated (n = 20, controls). After 4 or 12 weeks, AoC were explanted and analyzed by histology, immunohistology, and polymerase chain reaction. Pioglitazone significantly decreased the expression of inflammatory markers and reduced the macrophage-mediated inflammation in PIO compared with controls after 4 (P = 0.03) and 12 weeks (P = 0.012). Chondrogenic transformation was significantly decreased in PIO after 12 weeks (P = 0.001). Calcification of the intima and media was significantly reduced after 12 weeks in PIO versus controls (intima: P = 0.008; media: P = 0.025). Moreover, echocardiography revealed significantly better functional outcome of the AoC in PIO after 12 weeks compared with control. Interestingly, significantly increased intima hyperplasia could be observed in PIO compared with controls after 12 weeks (P = 0.017). Systemic PPAR-gamma activation prevents inflammation as well as intima and media calcification in AoC and seems to inhibit functional impairment of the implanted aortic valve. To further elucidate the therapeutic role of PPAR-gamma regulation for graft durability, translational studies and long-term follow-up data should be striven for.

Received for publication April 1, 2021; accepted September 25, 2021.

From the Department of Cardiac Surgery and Research Group for Experimental Surgery, Heinrich Heine University, Medical Faculty, Duesseldorf, Germany.

The authors report no conflicts of interest.

Supplemental digital content is available for this article. Direct URL citations appear in the printed text and are provided in the HTML and PDF versions of this article on the journal's Web site (www.jcvp.org).

Correspondence: Artur Lichtenberg, Department of Cardiovascular Surgery and Research Group for Experimental Surgery, Heinrich Heine University, Medical Faculty, Moorenstrasse 5, Duesseldorf 40225, Germany (e-mail: artur.lichtenberg@med.uni-duesseldorf.de).

Key Words: PPAR-gamma, calcification, degeneration, cardiovascular grafts

(*J Cardiovasc Pharmacol*™ 2022;79:103–115)

INTRODUCTION

Aortic valve replacement (AVR) for severe stenosis is a standard procedure in modern cardiovascular medicine. Biological valve prostheses have become the primary choice of patients undergoing AVR, almost irrespective of age at the time of operation. Continuous development and improvements as well as technological advances combined with minimally invasive techniques have made biological protheses more popular than ever. However, biological prostheses have several limitations, particularly in young patients, where rapidly calcifying processes with graft degeneration and final implant failure limit long-term outcome.[1,2] Degenerative deterioration of biological prostheses mainly occurs because of inflammatory processes.[3] The adaptive immunity has been described to cause implant failure in animals[4,5] and in humans.[6,7] Especially younger patients show accelerated degeneration, resulting in redo operations accompanied with increased risk of mortality.[8,9]

Therefore, optimization of the graft durability by inhibition of the implant degeneration is an important research focus. Previously, it has been demonstrated that activation of the peroxisome proliferator-activated receptor gamma (PPAR-gamma) can reduce inflammatory processes in vitro.[10–12] Pioglitazone, a PPAR-gamma agonist, was shown to decrease the degeneration of native aortic valves.[13] Still unanswered is the question whether PPAR-gamma activation also has an impact on inflammatory and degenerative processes in biological cardiovascular prostheses, which may have wide therapeutic implications. In a pilot study, Teshima et al[14] suggested that pioglitazone might have protective effects on biological prostheses.

In this study, we aim to examine the impact of systemic pioglitazone treatment on inflammation and degenerative calcification of aortic valve conduits (AoC) in a standardized rat model of heterotopic implantation.[15–18]

MATERIAL AND METHODS

Animals

Male Wistar rats were obtained from the local animal care facility of the Heinrich Heine University of Duesseldorf,

Germany. Male Sprague-Dawley rats were purchased from Janvier Labs (France). Every experiment was conducted according to the "Guide for the Care and Use of Laboratory Animals" and approved by the state animal care committee (reference number 84-02.04.2017.A182). In all surgical procedures, anesthesia and analgesia were secured by inhaled isoflurane (2.0%–2.5%) and intraperitoneally administered carprofen (5 mg/kg/d). Male Sprague-Dawley rats (n = 40, 200–250 g, 8 weeks old) were used as aortic conduit graft donors, and Wistar rats (n = 40, 200–250 g, 8 weeks old) served as recipients. Two different strains of rats are necessary to create a situation of allogenic transplantation, which is equivalent to the clinical scenario of homograft implantation.

All rats were fed ad libitum with a standard chow or an experimental diet. In group PIO (n = 20), pioglitazone 75-mg/kg chow (from ground up pill Actos, Takeda Pharma, with following ingredients: pioglitazone hydrochloride, lactose monohydrate, hydroxypropylcellulose, carboxymethylcellulose, and calcium and magnesium stearate) was additionally administered starting with the implantation of the AoC and continued until graft explantation. The dosage was chosen according to several previously published studies in rats.[19–22] Animals without pioglitazone treatment (n = 20) served as controls. Four weeks (short-term experiment) or 12 weeks (long-term experiment) after implantation, rats were examined with Doppler sonography evaluating the integrity of the graft. Explanted grafts were used for histology, immunohistology (n = 4 per group and time point), and quantitative real-time polymerase chain reaction (RT-PCR) (n = 6 per group and time point).

Creation of Aortic Valve Insufficiency

Native aortic valve insufficiency (AI) was created under echocardiographic guidance in all recipient rats as published before.[23] In brief, Wistar rats were anesthetized with isoflurane (2%–2.5%), and the right common carotid artery was exposed. A cannula was placed into the carotid artery through which a guide wire was inserted toward the aortic valve. The aortic valve leaflets were perforated with the guide wire under echocardiographic control (Philips HDX11) to generate an insufficiency grade II–III (Figs. 1A–E). Animals with AI grade I or IV were excluded from the experiment. The intention of generating an AI in the native aortic valve is to yield an improved hemodynamic situation for the implanted AoC with optimized implant valve functionality.[23]

Graft Harvesting

AoC were harvested from Sprague-Dawley rats (n = 40). Coronary arteries were ligated (Fig. 1F), and supra-aortic branches were clipped to avoid leakage after implantation. Afterward, conduits were cryopreserved under controlled conditions and stored at −80°.[18]

Heterotopic Graft Implantation and Explantation Procedures

Two weeks after the induction of native aortic valve insufficiency, donor AoC were infrarenally implanted into the recipient rat as previously described (Fig. 1G).[15,23] Briefly, Wistar rats were anesthetized, and after median laparotomy, the donor AoC were implanted into the infrarenal aorta in an end-to-side manner. Finally, the native aorta between the 2 anastomotic sites was ligated to guarantee maximum perfusion of the implanted graft. AoC perfusion was confirmed by Doppler sonography before wound closure.

Four or 12 weeks after implantation, animals were anesthetized as described above, and the integrity of the implanted AoC was again evaluated before explantation. After median laparotomy, systemic heparin administration by cannulation of the inferior caval vein was conducted. The implanted AoC were harvested, immediately rinsed with heparinized phosphate buffered saline, and processed for further examination.

Blood Plasma Analysis

Blood was taken after 4 (n = 20) or 12 weeks (n = 20), at the time point of explantation. Serum levels of calcium, phosphate, creatinine, urea, uric acid, cholesterol, and triglycerides were analyzed at the Institute of Clinical Chemistry and Laboratory Diagnostics, Medical Faculty, Heinrich Heine University, Duesseldorf, Germany, applying commercially available standard assays designed for an automated clinical chemistry analyzer (series Cobas, Roche, Basel, Switzerland).

Histology

Cryosections were used to perform histology. The following stainings were analyzed: hematoxylin–eosin (H.E.) staining, Movat's pentachrome staining, von Kossa staining, and Alizarin Red staining. Morphometric analyses for the detection of intergroup differences were performed using ImageJ (Wayne Rasband; National Institutes of Health, Bethesda, MD). To compare intima hyperplasia, a standardized scoring system was used as previously published.[16] In brief, explanted AoC were divided into 4 regions: region A1 (aortic valve region), region A2 (ascending aorta), region B1 (descending aorta), and region B2 (descending aorta with distal anastomosis (Fig. 1H)). In each region, 3 cross sections were analyzed, and each cross section was divided into 8 segments in which the intima and media thickness was measured to determine the mean intima-to-media ratio. All histological examinations were single-blinded during the study period.

For quantification of the calcification of the explanted grafts, a recently published scoring system was used but slightly modified.[17] Therefore, the graft was also divided into 4 regions as described above. From each region, cross sections were divided into 4 segments in which the scoring system was conducted. For the intima and media, the scoring range was 0–5, that is, 0 = no calcification; 1 = microcalcification; 2 = mild calcification, brown discoloration; 3 = macrocalcification $<$50% of the intima/media; 4 = macrocalcification 50%–75% of the intima/media; and 5 = macrocalcification $>$75% of the intima/media, resulting in maximum values of 20. An additional analysis of the calcification was performed by using Alizarin Red staining. Again, each graft was divided into 4 regions, and one cross section of each region was used. Calcified areas were measured and divided by the area of the intima and media using Fiji (by ImageJ).

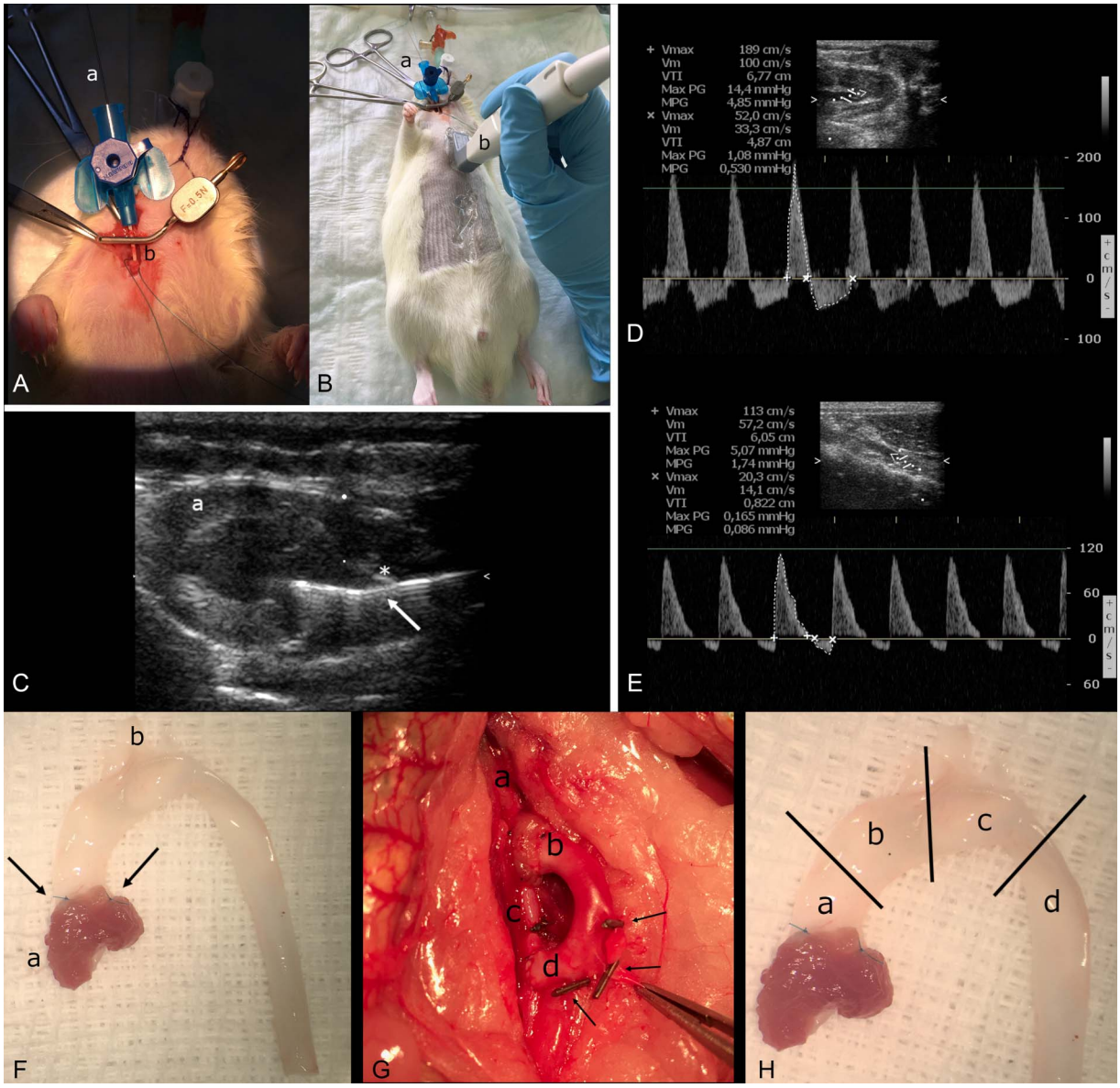

FIGURE 1. Experimental set-up of the heterotopic AoC implantation. A, Insertion of the cannula together with the guide wire into the right carotid artery. a, guide wire; b, right carotid artery. B, Echocardiographic control of AI generation. a, guide wire; b, ultrasound probe. C, Induction of AI with a guide wire. →, guide wire; *, aortic valve; a, left ventricular myocardium. D, Echocardiographic control of AI by measuring the severity of AI in the ascending aorta. VTI, velocity-time integral. E, Measurement of the relative retrograde diastolic flow in the abdominal aorta. F, Harvested aortic conduit; a, aortic valve; b, supra-aortic branches; →, ligated coronary arteries. G, Infrarenally implanted aortic valve conduit; a, abdominal aorta; b, proximal anastomosis of the conduit; c, ligated native aorta; d, distal anastomosis of the conduit; →, ligated supra-aortic branches. H, Division of the conduit in 4 regions; a, aortic valve region (A1); b, ascending aorta (A2); c, descending aorta (B1); and d, descending aorta with distal anastomosis (B2). AI, aortic valve insufficiency.

Immunohistology

For immunohistology, cryosections (5 μm) from each region were incubated at room temperature for 10 minutes with 0.25% Triton X-100 and for 1 hour with 5% bovine serum albumin +0.1% Tween-20. Incubation with primary antibodies [anti-von Willebrand (vWF) factor (1:300; A0082, DAKO, Hamburg, Germany); anti–alpha-smooth muscle actin (αSMA) (1:300; A5228, Sigma-Aldrich, Taufkirchen, Germany); anti-syndecan-3 (1:100; ab63932, Abcam, Cambridge, United Kingdom); anti-CD3 (1:300; C7930, Sigma-Aldrich); anti-CD68 (1:200; ab31630, Abcam); anti-CD163 (1:200; ab182422, Abcam); and anti-receptor for advanced glycation end products (RAGE) (1:100; ab3611, Abcam)] + 1% bovine serum albumin +0.1% Tween-20 lasted 1 hour at 37°C. Secondary antibodies conjugated to the fluorophores Alexa488 (1:200; A11070,

Invitrogen, Carlsbad, CA) and Alexa546 (1:200; A11030, Invitrogen) were applied (in phosphate buffered saline containing 1% bovine serum albumin and 0.1% Tween-20) for 45 minutes in a dark and humid chamber at 37°C. For counterstaining, cryosections were incubated with 4′,6-diamidino-2-phenylindole (DAPI) (Roth, Karlsruhe, Germany) for 5 minutes in a dark and humid chamber. Afterward, sections were covered with Leica medium (Leica Biosystems, Nussloch, Germany), and image acquisition was conducted with a microscope system DM2000, equipped with a digital camera DFC 425C (Leica, Wetzlar, Germany) and the Leica Application Suite V3.7 software.

For syndecan-3 staining, representative sections of each region of the explanted conduit were analyzed according to the following categorical scoring system: 0 = no signal; 1 = single spots; 2 = moderate accumulation; and 3 = extensive accumulation. For semiquantitative evaluation of CD3- and CD68-positive cells, 4 representative sections of each region of the conduit were analyzed as follows: In each section, all CD3- or CD68-positive cells were counted and divided by all DAPI-positive cells, so that the relative amount of CD3 and CD68 cells was determined. For semiquantitative evaluation of CD68- and CD163-positive cells, 4 representative sections of each conduit were analyzed as follows: In each section, all CD68- and CD163-positive cells were counted and divided by all CD68-positive cells. For semiquantitative evaluation of RAGE-positive cells, 4 representative sections of each region of the conduit were analyzed as follows: In each section, all RAGE-positive cells were counted and divided by all DAPI-positive cells. This analysis was conducted automatically with Fiji (by ImageJ).

Quantitative RNA Analysis

Quantitative RT-PCR was performed to analyze marker gene expressions in the explanted AoC. Total RNA was isolated using a commercially available kit (RNeasy Mini Kit, Qiagen, Hilden, Germany). In brief, tissue was homogenized in TRIzol (Sigma-Aldrich, Steinheim, Germany), and RNA was precipitated by isopropanol. To conduct quality analyses, RNA samples were collected after passaging through a DNA-removing column (Qiagen, Hilden, Germany). Quantity and purity of the isolated RNA were determined spectrophotometrically (BioPhotometer plus; Eppendorf, Hamburg, Germany), and optical density values at 230, 260, and 280 nm were recorded. Furthermore, to detect the level of RNA degradation, the Agilent RNA 6000 Nano Kit (Agilent Technologies, Santa Clara, CA) was used. Total cDNA was generated using QuantiTect Reverse Transcription Kit (Qiagen, Hilden, Germany) according to the manufacturer's recommendation. Quantitative RT-PCR was conducted on a StepOnePlus cycler (Applied Biosystems, Foster City, CA) using the Platinum SYBR Green PCR Master Mix (Invitrogen, Darmstadt, Germany) with a reaction volume of 20 μL: 50°C for 2 minutes, 95°C for 2 minutes, 95°C for 15 seconds and 60°C for 30 seconds (40 cycles), 95°C for 15 seconds, 60°C for 1 minute, 95°C for 15 seconds, and 60°C for 15 seconds.

Relative gene expression was determined using the δδCt method and RPL13a as a housekeeping gene. Primers for the following genes were obtained from Invitrogen: inflammation-associated genes [tumor necrosis factor-alpha (TNF-α); interleukin-1 beta (IL-1β); interleukin-6 (IL-6); and receptor for advanced glycation end products (RAGE)], genes associated with vascular degeneration and chondro-osteogenic transformation [osteopontin (OPN); osteocalcin (OCN)], and transcription factors associated with osteogenic differentiation [bone morphogenetic protein-2 (BMP2); runt-related T1 transcription factor-2 (RUNX2)]. In Table 1, all primer sequences are presented.

Echocardiographic Analysis

The severity of native aortic valve insufficiency (AI) was determined as previously published.[23] In brief, the ratio of blood velocity across the period of diastole [velocity-time integral (VTI)-II] divided by the blood velocity across the period of systole (VTI-I) was measured in the ascending aorta (Fig. 1D).[23] Ratio values of 0.5–0.7 were defined as AI grade II-III. In addition, to be sure to have a sufficient reversed diastolic flow in the abdominal aorta, the ratio of VTI-II/VTI-I in the abdominal aorta was calculated (Fig. 1E).

Statistics

Variables are shown as mean ± SEM. Group comparisons were conducted by unpaired Student's *t* tests with or without Welch's correction or Mann–Whitney *U* tests, as indicated. $P < 0.05$ was assumed to indicate significance. Data analysis was conducted with GraphPad Prism 6 (GraphPad Software, San Diego, CA).

TABLE 1. Primer Sequences for Quantitative RT-PCR

Gene	Forward Sequence	Reverse Sequence
BMP2	5′-GCTCAGCTTCCATCACGAA-3′	5′-AAGAAGCGTCGGGAAGTTTT-3′
IL-1β	5′-AGGACCCAAGCACCTTCTTT-3′	5′-CATCATCCCACGAGTCACAG-3′
IL-6	5′-ACCACCCACAACAGACCAGT-3′	5′-AGTGCATCATCGCTGTTCAT-3′
OPN	5′-AAGCCTGACCCATCTCAGAA-3′	5′-ATGGCTTTCATTGGAGTTGC-3′
OCN	5′-AAGCAGGAGGGCAGTAAGGT-3′	5′-GTCCGCTAGCTCGTCACAAT-3′
RAGE	5′-TGAACTCACAGCCAATGTCC-3′	5′-TCAGAGGTTTCCCATCCAAG-3′
RUNX2	5′-GATGACACTGCCACCTCTGA-3′	5′-GATGAAATGCCTGGGAACTG-3′
TNF-α	5′-GCTCCCTCTCATCAGTTCCA-3′	5′-GCTTGGTGGTTTGCTACGAC-3′

RESULTS

Weight and Food Intake Follow-up

In the short-term and in the long-term experiment, no differences between the 2 groups could be shown regarding gain of weight during the follow-up. All rats gained weight adequately [weight gain in the short-term experiment (in gram): 179.7 ± 17.32 vs. 173.5 ± 13.48; $P = 0.78$. Weight gain in the long-term experiment (in gram): 269.7 ± 26.87 vs. 290.7 ± 20.39; $P = 0.54$]. Food intake was similar in both groups, although after implantation, all rats showed a reduced intake, which was normalized again after 2 weeks (see **Fig. 1A+B**, **Supplemental Digital Content 1**, http://links.lww.com/JCVP/A714, which demonstrates the food intake).

Operative and Functional Results

The functional results of the induction of the AI were comparable between the treatment groups PIO and control. In both follow-up period groups (4 weeks and 12 weeks), both treatment groups showed similar severity of native aortic valve insufficiency and relative retrograde diastolic flow in the abdominal aorta at the time point of AI induction (see **Fig. 1C**, **Supplemental Digital Content 1,** http://links.lww.com/JCVP/A714, which shows the echocardiographic results). AI severity remained stable and comparable between both treatment groups until the time point of graft implantation (see **Fig. 1D**, **Supplemental Digital Content 1**, http://links.lww.com/JCVP/A714, which shows the echocardiographic results).

The overall operation time for the implantations was similar in both groups (in minutes: 71.5 ± 1.6 vs. 71.5 ± 1.8; $P = 0.7$). The clamping time to suture the AoC was also similar in both groups (clamping time of the proximal anastomosis in minutes: 23.7 ± 0.6 vs. 22.3 ± 0.5; $P = 0.6$; clamping time of the distal anastomosis in minutes: 15.7 ± 0.3 vs. 16.1 ± 0.5; $P = 0.2$). VTI ratio measurements distal to the implanted AoC revealed no diastolic retrograde flow indicating competence of the donor aortic valves of all implants (see **Fig. 1D**, **Supplemental Digital Content 1**, http://links.lww.com/JCVP/A714, which shows the echocardiographic results).

Until the time of explantation, the severity of native AI remained comparable between the 2 groups after 4 weeks and after 12 weeks (Fig. 5K, L).

Inflammatory Activity in Aortic Valve Conduits

The inflammatory activity was assessed by immunohistology and quantitative RNA analysis. No differences could be shown for CD3 staining neither after 4 weeks nor after 12 weeks (Figs. 2A–C). CD68 was significantly decreased in PIO compared with controls after 4 weeks ($P = 0.03$) and after 12 weeks ($P = 0.012$) (Figs. 2A, B, D). The ratio of CD68- and CD163-positive cells to CD68-positive cells was similar in both groups at both time points (Figs. 2E–G). IL-6 gene expression was significantly decreased after 12 weeks in group PIO compared with group control ($P = 0.015$) (Fig. 2H). Furthermore, in group PIO, a significantly decreased IL-6 gene expression could be observed after 12 weeks compared with the short-term experiment ($P = 0.04$) (Fig. 2H). There was a tendency of reduced IL-1β gene expression after 4 weeks ($P = 0.06$) and 12 weeks ($P = 0.09$) in PIO compared with controls but without a statistical significance (Fig. 2K). TNF-α gene expression showed no differences between PIO and controls after 4 weeks but was significantly increased in group PIO after 12 weeks ($P = 0.009$) (Fig. 2L). No differences occurred between both groups concerning RAGE gene expression (Fig. 2M). No intergroup differences could be shown for RAGE staining neither after 4 nor after 12 weeks (see **Fig. 2A-E**, **Supplemental Digital Content 2**, http://links.lww.com/JCVP/A715, which demonstrates the RAGE activation in aortic valve conduits).

Osteochondrogenic Degeneration in Aortic Valve Conduits

Intima hyperplasia assessed by an intima-to-media ratio (IMR) in H.E. staining showed no differences after 4 weeks (see **Fig. 3**, **Supplemental Digital Content 3**, http://links.lww.com/JCVP/A716, which demonstrates the assessment of intima hyperplasia and cellular composition by H.E. and αSMA/vWF staining). After 12 weeks, significantly increased intima hyperplasia could be shown in PIO compared with controls ($P = 0.017$) (see **Fig. 3E**, **Supplemental Digital Content 3**, http://links.lww.com/JCVP/A716, which shows the assessment of the intima hyperplasia). αSMA and vWF staining showed ubiquitary αSMA expression in the hyperplastic intimal regions and in the implant media and vWF-positive endothelial cells on the luminal side (see **Fig. 3F-K**, **Supplemental Digital Content 3**, http://links.lww.com/JCVP/A716, which demonstrates the assessment of intima hyperplasia and cellular composition by H.E. and αSMA/vWFstaining).

The Movat's pentachrome staining was assessed to focus on osteochondrogenic transformation. In this staining, musculature occurs red-blue, reticular connective tissue and collagen appears yellow, fibrin in red, cell nuclei and elastic fibers in black, and glycosaminoglycans in green-blue. Detection of glycosaminoglycans indicates the existence of chondrocytes and therefore chondrogenic transformation. In the short-term experiment, only in the A1 region in PIO and controls, a slight green-blue staining could be observed (Fig. 3). In the long-term experiment, a more intensive green-blue staining could be demonstrated in all regions in controls compared with PIO (Fig. 3).

Pioglitazone administration significantly reduced chondrogenic transformation, as assessed by syndecan-3 staining after 12 weeks ($P = 0.001$) (Fig. 4A). Particularly, in the implant, media cells with a chondrogenic phenotype were colocalized with syndecan-3 (Figs. 4B, C).

OPN gene expression was significantly decreased after 12 weeks under pioglitazone treatment ($P = 0.002$) (Fig. 4D). Furthermore, OPN was significantly decreased in PIO after 12 weeks compared with 4 weeks ($P = 0.004$) (Fig. 4D). Also, OCN gene expression was significantly decreased after 12 weeks in PIO ($P = 0.015$) (Fig. 4E). In group PIO, a significantly decreased OCN gene expression occurred after 12

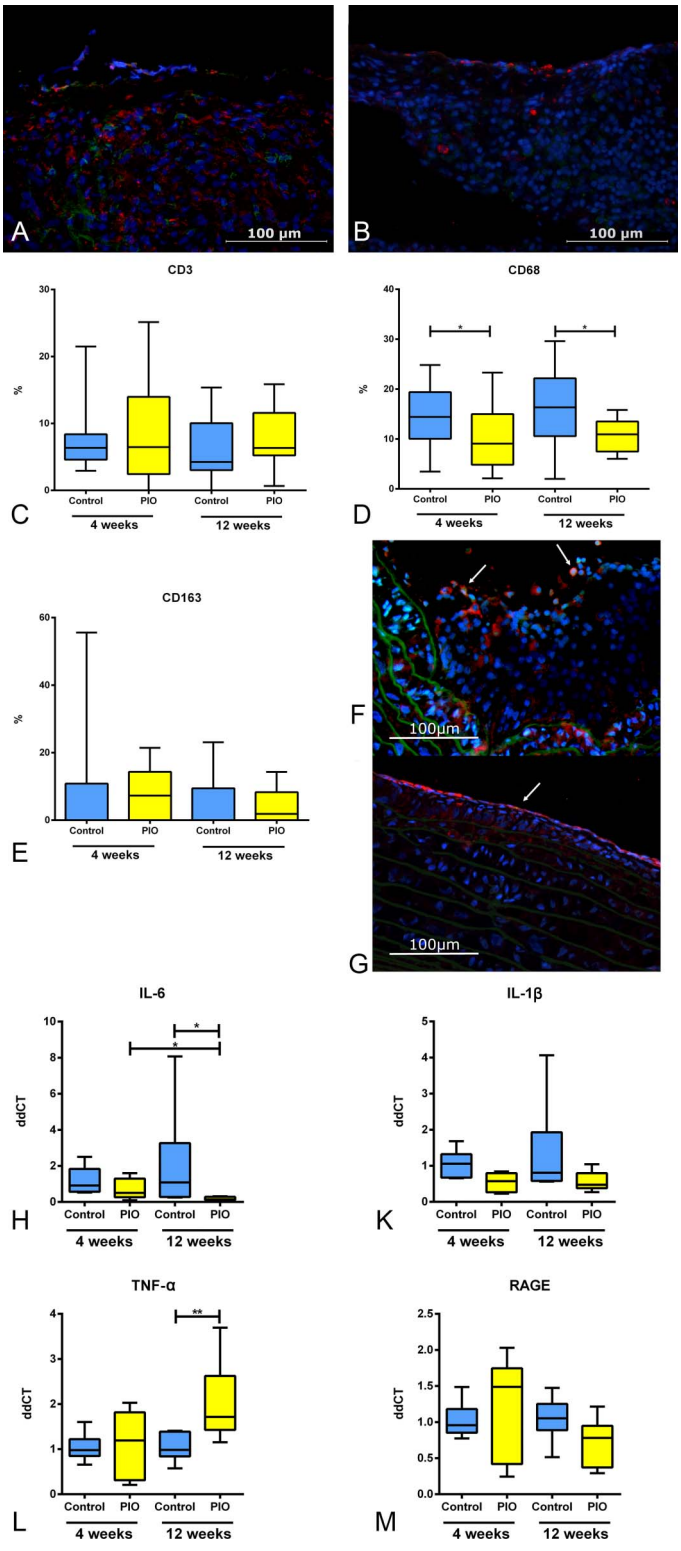

FIGURE 2. Inflammatory activity in aortic valve conduits. Inflammatory activity assessed by CD3/CD68 staining. Exemplary CD3 (green) and CD68 (red) staining of control after 12 weeks (A) and group PIO after 12 weeks (B). Ratio of CD3-positive cells to all cells in % after 4 weeks (n = 8) and 12 weeks (n = 8) (C). Ratio of CD68-positive cells to all cells in % after 4 weeks (n = 8) and 12 weeks (n = 8) (D). Ratio of CD68- and CD163-positive cells to CD68-positive cells in % after 4 weeks (n = 8) and 12 weeks (n = 8) (E). Exemplary CD163 (green) and CD68 (red) staining of PIO after 12 weeks (F) and control after 12 weeks (G). →, CD68- and CD163-positive cells. Significantly higher expression of CD68 cells (red) in controls compared with PIO is observed, whereas CD3 cells (green) show no differences. The ratio of M1 and M2 macrophages is similar in both groups at both time points. Inflammatory gene expression: IL-6, IL-1β, TNF-α, and RAGE. IL-6 gene expression after 4 weeks (n = 12) and 12 weeks (n = 12) (H). IL-1β gene expression after 4 weeks (n = 12) and 12 weeks (n = 12) (K). TNF-α gene expression after 4 weeks (n = 12) and 12 weeks (n = 12) (L). RAGE gene expression after 4 weeks (n = 12) and 12 weeks (n = 12) (M). IL-6, interleukin-6; IL-1β, interleukin-1 beta; TNF-α, tumor necrosis factor-alpha; RAGE, receptor for advanced glycation end products. $*P < 0.05$; $**P < 0.01$.

weeks compared with 4 weeks ($P = 0.004$) (Fig. 4E). On the level of transcription factors, the 2 analyzed osteogenic markers BMP2 and RUNX2 were unaltered (Fig. 4F, G). Pioglitazone treatment showed significantly decreased BMP2 levels after 12 weeks compared with four weeks ($P = 0.015$) (Fig. 4F).

Calcification was assessed by Alizarin Red and von Kossa staining. Alizarin Red staining revealed

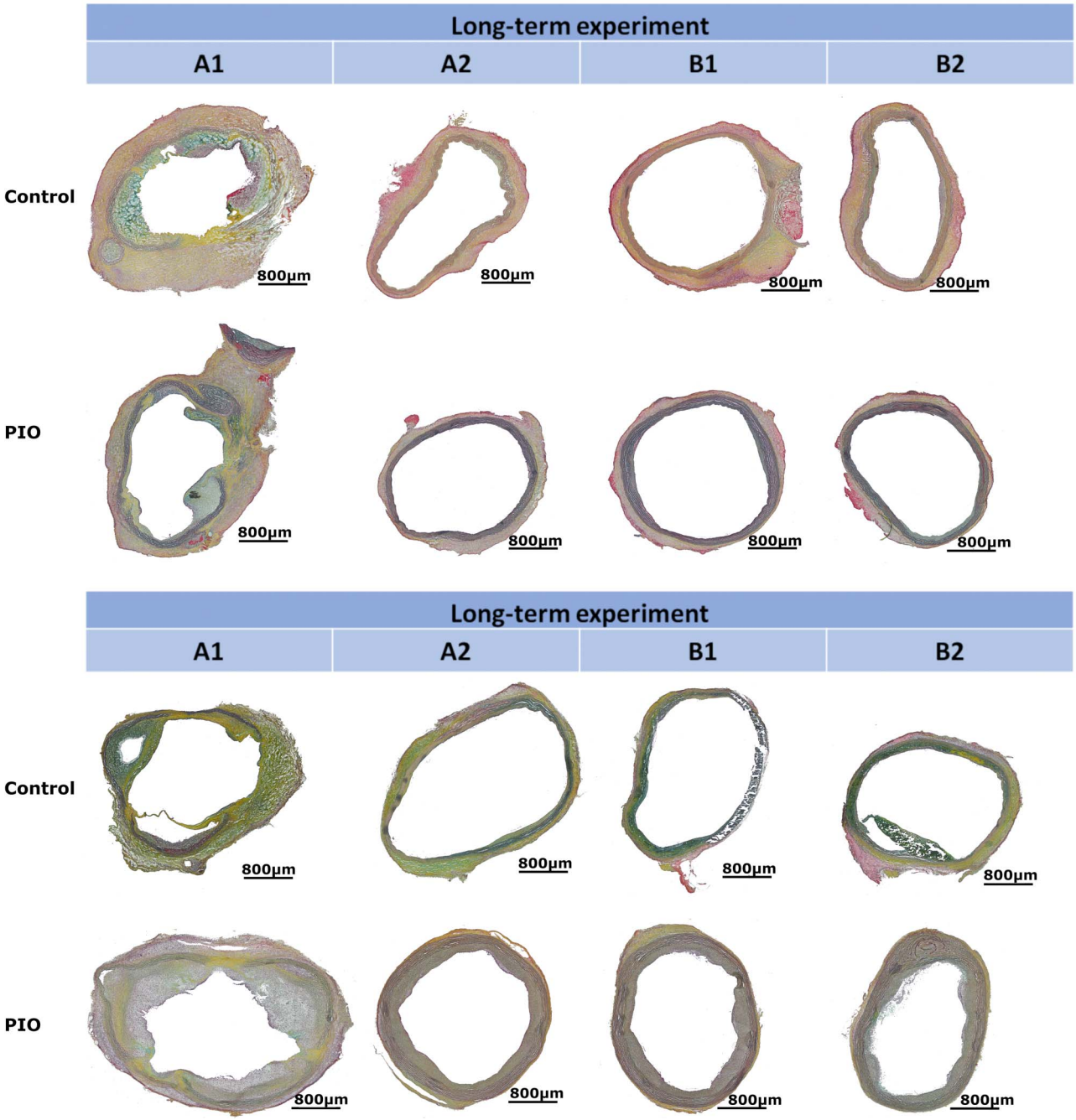

FIGURE 3. Histomorphological overview on AoC explants. Exemplary Movat's pentachrome staining of group control and PIO in the short- and long-term experiment. In this staining, musculature occurs red-blue, reticular connective tissue and collagen appears yellow, fibrin in red, cell nuclei and elastic fibers in black, and glycosaminoglycans in green-blue. Detection of glycosaminoglycans indicates the existence of chondrocytes and therefore chondrogenic transformation. In the long-term experiment, a more intensive green-blue staining could be demonstrated in all regions in controls compared with PIO.

significantly decreased calcification after 12 weeks in PIO compared with controls ($P = 0.029$) (Fig. 5A–C). After 4 weeks, no differences were detected between the 2 groups (Fig. 5C). In the control group, significantly increased calcification could be observed after 12 weeks compared with 4 weeks ($P = 0.029$) (Fig. 5C). von Kossa staining revealed that after 4 weeks in vivo, no differences could be shown in the intima (Fig. 5G). However, pioglitazone significantly decreased intima calcification in donor AoC after 12 weeks ($P = 0.008$) (Fig. 5D, F, G). Media

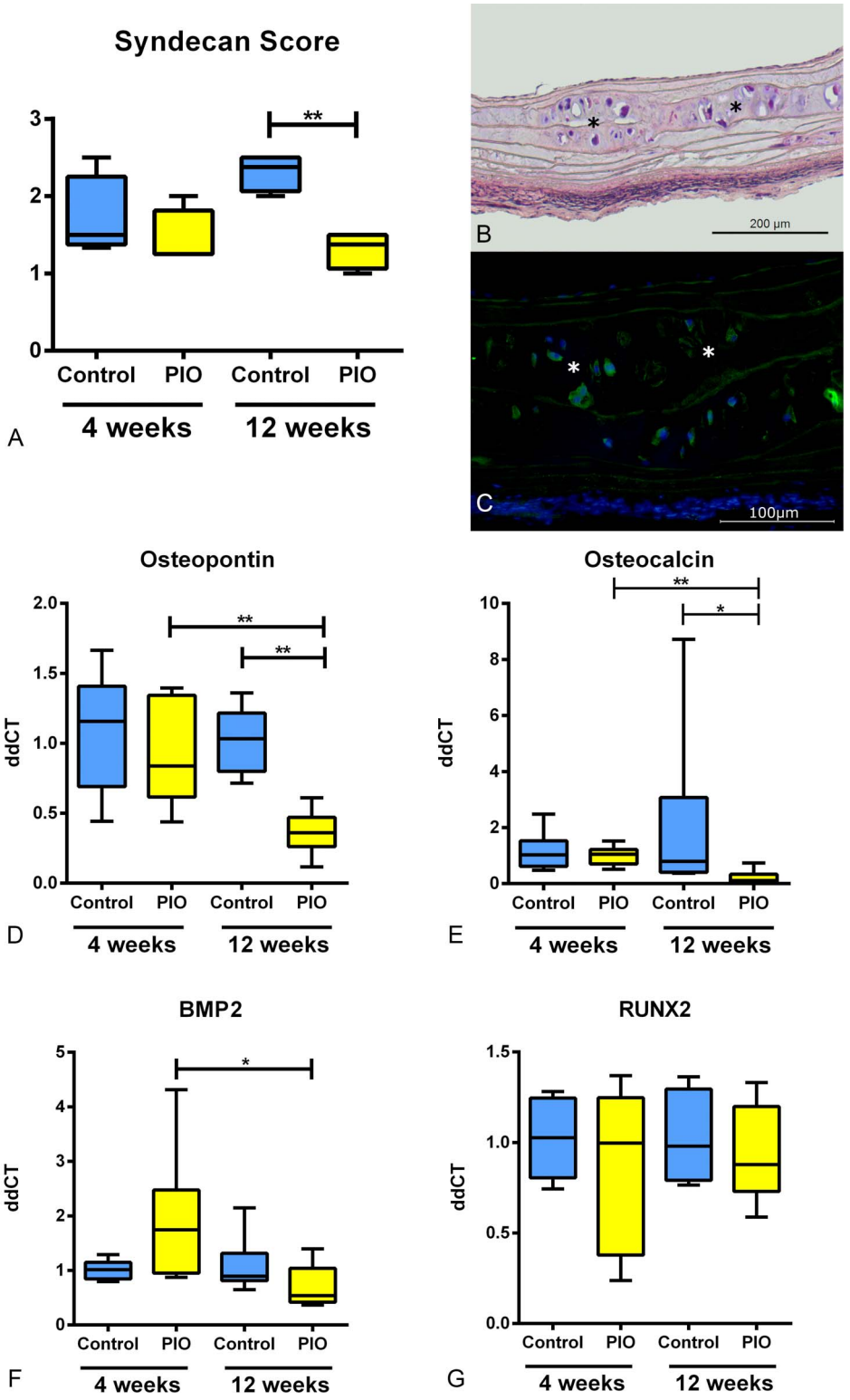

FIGURE 4. Osteochondrogenic transformation in aortic valve conduits. Syndecan-3. Syndecan score after 4 weeks (n = 8) and 12 weeks (n = 8) (A). *, Chondrogenic cells in H.E. B, And, syndecan-3 staining (C). Chondrogenic transformation gene expression: osteopontin gene expression after 4 (n = 12) and 12 weeks (n = 12) (D). Osteocalcin gene expression after 4 (n = 12) and 12 weeks (n = 12) (E). BMP2 gene expression after 4 (n = 12) and 12 weeks (n = 12) (F). RUNX2 gene expression after 4 (n = 12) and 12 weeks (n = 12) (G). BMP2, bone morphogenetic protein-2; RUNX2, runt-related T1 transcription factor-2. *$P < 0.05$; **$P < 0.01$.

calcification was also significantly decreased after 12 weeks in PIO versus controls ($P = 0.025$) (Fig. 5E, F, H). After 4 weeks, no differences occurred comparing PIO and controls (Fig. 5H).

There were no differences concerning the functionality of the donor AoC after 4 weeks (Fig. 5K). After 12 weeks, valvular insufficiency of donor AoC was significantly lower in group PIO compared with group control ($P = 0.001$) (Fig. 5L).

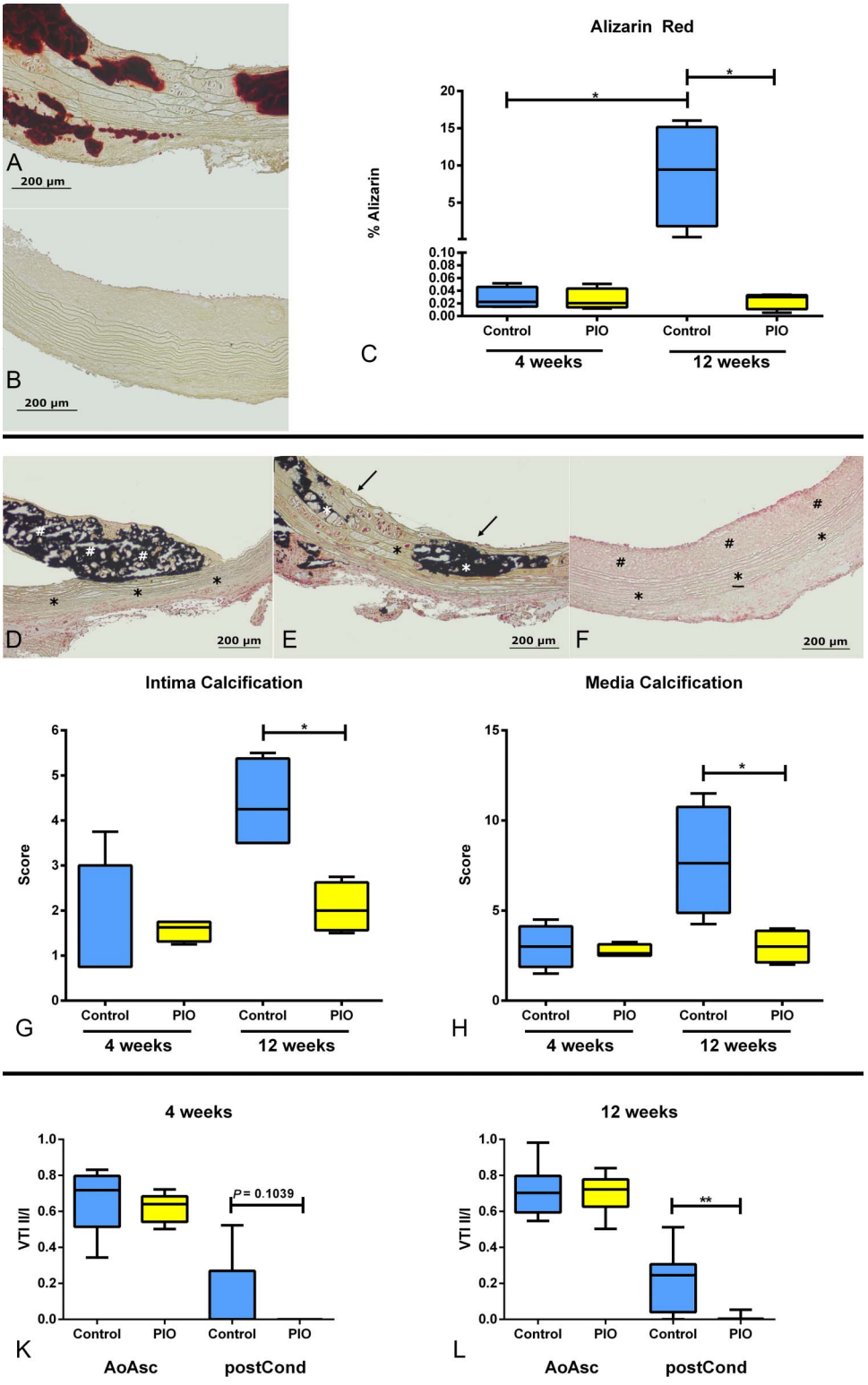

FIGURE 5. Calcification of the aortic valve conduits. Exemplary Alizarin Red staining of a calcified region of controls after 12 weeks (A) and noncalcified region of PIO after 12 weeks (B). Area of Alizarin Red compared with area of intima and media after 4 (n = 8) and 12 weeks (n = 8) (C). Exemplary von Kossa staining of a severely calcified intima region of the graft of the controls after 12 weeks (D); #, intima, *, media. Media calcification in detail (E); →, intima; *, media. Exemplary von Kossa staining of a slightly calcified region of the graft of group PIO after 12 weeks (F); #, intima; *, media. Intima calcification after 4 (n = 8) and 12 weeks (n = 8) (G). Media calcification after 4 (n = 8) and 12 weeks (n = 8) (H). Echocardiographic data (VTI ratios VTI-II/VTI-I) at the time point of explantation after 4 weeks (n = 20) (K) and after 12 weeks (n = 20) (L). postCond, abdominal aorta distally of the implanted conduit. $*P < 0.05$; $**P < 0.01$.

Blood Plasma Analysis

Decreased calcium levels could be shown in PIO compared with controls after 4 weeks ($P = 0.034$) (see **Fig. 4A**, **Supplemental Digital Content 4**, http://links.lww.com/JCVP/A717, which shows the blood plasma analysis); however, this difference was lost after 12 weeks (see **Fig. 4A, Supplemental Digital Content 4**, which shows the blood plasma analysis). Phosphate levels

were similar after 4 and 12 weeks in both groups (see **Fig. 4A**, **Supplemental Digital Content 4**, http://links.lww.com/JCVP/A717, which shows the blood plasma analysis). Creatinine, urea, and uric acid levels were comparable after 4 weeks comparing PIO with control (see **Fig. 4B**, **Supplemental Digital Content 4**, http://links.lww.com/JCVP/A717, which shows the blood plasma analysis). Significantly increased creatinine levels occurred in group control after 12 weeks compared with 4 weeks ($P = 0.003$) and in group PIO after 12 weeks compared with 4 weeks ($P = 0.012$) (see **Fig. 4B**, **Supplemental Digital Content 4**, http://links.lww.com/JCVP/A717, which shows the blood plasma analysis). After 12 weeks, significantly lower creatinine levels were observed in PIO compared with controls ($P = 0.04$) (see **Fig. 4B**, **Supplemental Digital Content 4**, http://links.lww.com/JCVP/A717, which shows the blood plasma analysis). Significantly increased uric acid levels could be seen in control after 12 weeks compared with control after 4 weeks ($P = 0.002$) (see **Fig. 4B**, **Supplemental Digital Content 4**, http://links.lww.com/JCVP/A717, which shows the blood plasma analysis). Furthermore, uric acid was significantly decreased in PIO compared with controls ($P = 0.01$) (see **Fig. 4B**, **Supplemental Digital Content 4**, http://links.lww.com/JCVP/A717, which shows the blood plasma analysis). No differences could be detected for urea levels in both groups after 12 weeks (see **Fig. 4B**, **Supplemental Digital Content 4**, http://links.lww.com/JCVP/A717, which shows the blood plasma analysis). Cholesterol levels were similar in both groups after 4 and 12 weeks (see **Fig. 4C**, **Supplemental Digital Content 4**, http://links.lww.com/JCVP/A717, which shows the blood plasma analysis). However, significantly increased cholesterol levels occurred in control after 12 weeks compared with 4 weeks ($P = 0.039$) (see **Fig. 4C**, **Supplemental Digital Content 4**, http://links.lww.com/JCVP/A717, which shows the blood plasma analysis). Pioglitazone administration diminished triglyceride levels after 4 weeks by trend ($P = 0.06$) (see **Fig. 4C**, **Supplemental Digital Content 4**, http://links.lww.com/JCVP/A717, which shows the blood plasma analysis). After 12 weeks, no differences could be shown comparing PIO with control (see **Fig. 4C**, **Supplemental Digital Content 4**, http://links.lww.com/JCVP/A717, which shows the blood plasma analysis).

DISCUSSION

In this study, the role of PPAR-gamma activation through pioglitazone administration for the prevention of cardiovascular graft degeneration was examined in a standardized small animal model.[15] In this in vivo study, PPAR-gamma activation reduced inflammation in valved aortic conduits, as demonstrated by a significantly decreased IL-6 gene expression and a reduced IL-1β gene expression. Especially IL-6 expression has been reported to be associated with enhanced inflammation and graft degeneration.[24] Several studies have described the anti-inflammatory activity of PPAR-gamma agonists in vitro[10–12,25] by reducing the expression of proinflammatory cytokines such as IL-1β and IL-6.[10] There is evidence, that PPAR-gamma activation can reduce IL-6 and IL-1β by antagonizing the activities of the transcription factors AP-1, STAT, and NF-kappaB.[11] In a previously published study by Ross et al, it could be demonstrated that macrophages play a crucial role in the development and progression of atherosclerosis.[26] Several animal models have delivered evidence for macrophages being a negative factor in cardiovascular degeneration.[27–29] Especially M1 macrophages are mainly involved in proinflammatory responses, whereas M2 macrophages rather have an anti-inflammatory role.[30–32] Ricote et al have shown that PPAR-gamma activation may counteract macrophage activation.[11] In this study, pioglitazone administration also decreased macrophage infiltration in the short- and long-term experiment, supporting the antidegenerative effect of pioglitazone, as the ratio of M2 to M1 macrophages was unaffected.

However, T-cell regulation was not affected by pioglitazone. This is in contrast to a previously published study, suggesting that PPAR-gamma activation may reduce CD3 gene expression and therefore T-cell–dependent inflammation.[33] In that study, CD3 gene expression was analyzed in obese rats, showing a pathological glucose and insulin tolerance test. Furthermore, it has been shown that mice fed with high-fat diet exhibit a higher amount of T-cell infiltration when compared with animals on regular diet.[34] Thus, discrepant findings in our study might be explained by the fact that PPAR-gamma activation reduces CD3-positive cell infiltration in obese mice but probably has no relevant impact on T cells in rats under normal diet.

Surprisingly, TNF-α gene expression in the explanted aortic conduits was increased by pioglitazone after 12 weeks, which is in contrast to previously published studies, where Jiang et al showed that PPAR-gamma inhibits TNF-α in vitro in adipose tissue,[10] and Murakami-Nishida et al demonstrated that PPAR-gamma treatment decreased circulating TNF-α levels in Apoe$^{-/-}$ mice.[35] On the contrary, Zhang et al demonstrated that PPAR-gamma inhibitors attenuate TNF-α expression, and moreover, TNF-α stimulation upregulated the activity of PPAR-gamma.[36] It could be shown that early atherosclerosis induced by TNF-α could be reduced by PPAR-gamma inhibitors in a mouse model.[36] In line with the latter reports, our study revealed an upregulation of TNF-α gene expression in the grafts explanted from pioglitazone-treated animals. Although TNF-α is predominantly described to have proinflammatory activities, the entirety of molecular mechanisms is still not fully understood.

Another aspect of inflammation is represented by activation of RAGE, which has been previously described to enhance cardiovascular calcification in rats.[37] In this context, PPAR-gamma activation has been reported to downregulate RAGE, thereby attenuating degenerative processes in native vasculature.[13,19,38] Wang et al described an inhibition of RAGE through PPAR-gamma activation by inhibiting NF-kappaB.[39] In our study, the PPAR-gamma agonist pioglitazone had no impact on the expression of RAGE. Wei et al described an elevated level of AGE in aortic tissue in diabetic rats.[37] Also, Katz et al demonstrated that patients with

diabetes or metabolic syndrome have significantly higher AGE levels.[40] One can assume that in this study, no decrease of RAGE expression occurred because rats were under normoglycemic conditions with probably nonaugmented AGE levels. Moreover, there were no differences in RUNX2 and BMP2 gene expression. BMP2 is a pro-osteogenic factor that is known to be related to cardiovascular calcification.[41] RUNX2 is a transcription factor which is associated with the differentiation of osteoblasts.[42] Li et al could show that RAGE activation was associated with higher expression of BMP2 and RUNX2 and consequently increased osteoblastic differentiation of VICs.[13] It is likely that the absence of elevated RAGE levels explains why BMP2 and RUNX2 were not regulated in our model.

PPAR-gamma agonists have been reported to attenuate atherosclerosis of the native cardiovascular system in mouse models with a genetic predisposition.[43,44] These findings are further amplified by the insights from this study, suggesting that calcific degeneration of cardiovascular bioimplants is also inhibited by PPAR-gamma activation. Implant calcification as assessed by von Kossa staining and Alizarin Red staining was significantly decreased in pioglitazone-treated animals after 12 weeks. Calcification of the cardiovascular system is a degenerative process wherein calcium deposition is a passive mechanism.[45] Also, Li et al described significantly decreased calcium deposits as marker of cardiovascular calcification in hypercholesterolemic rabbits treated with pioglitazone.[13] In this study, we see decreased calcium concentrations in blood plasma under pioglitazone administration, which may hint at reduced circulating calcium supporting diminished graft calcification. Furthermore, in this study, osteopontin and osteocalcin gene expression were significantly reduced in pioglitazone-treated rats. Thus, osteogenic differentiation was significantly decreased through PPAR-gamma activation. These findings go in line with previously published studies. There is evidence that PPAR-gamma inhibits osteoblastic differentiation.[46] Lin et al showed that PPAR-gamma activation resulted in decreased osteocalcin expression.[46] It could be shown that PPAR-gamma knockout resulted in higher osteopontin induction in mice.[47,48]

In addition, early chondro-osteogenic transformation could be shown to be significantly diminished by PPAR-gamma as assessed by syndecan-3 staining.

In this study, we could show significantly decreased calcifying degeneration in the presence of increased intima hyperplasia. In contrast to our findings, PPAR-gamma agonists have been previously demonstrated to attenuate early atherosclerosis in animal models also by decreasing intima hyperplasia in carotid arteries.[49,50] Moreover, Minamikawa et al have demonstrated that PPAR-gamma agonists attenuate intima hyperplasia in patients.[51] We speculate that this difference may be related to the differing nature of the reports, considering that Minamikawa et al have studied patients suffering from type 2 diabetes mellitus as opposed to normoglycemic rats studied here. Despite the finding of increased intima hyperplasia, functional outcome of the implanted conduits in our study was not impaired. In fact, graft valve functionality proved superior with a significantly decreased graft valve insufficiency. Furthermore, in the absence of pioglitazone, hyperplastic intima areas seem to undergo rapid degeneration with early calcification, whereas pioglitazone-treated animals show decreased calcification.

Limitations of the Study

This study is an in vivo examination of the impact of pioglitazone in the context of degenerative calcification of cryopreserved valved aortic grafts. According to our experience with different small animal implantation models, rats are the smallest animals that can be used to perform the microsurgical implantation of functional aortic valve conduits effectively and safely. However, the presented rat model does not entirely mimic the complexity of degenerative processes that act on cardiovascular protheses in the clinical setting. Typical comorbidities from which most patients suffer, such as obesity, diabetes, uremia, or hypercholesterolemia, are not included in our model. Therefore, we will conduct further preclinical studies integrating frequent cardiovascular comorbidities, such as hypercholesterolemia or diabetes, and in the following, large animal model studies will be considered. Interestingly, blood plasma analyses of this study showed slightly, but yet significantly lower creatinine levels after 12 weeks in group PIO. Although a nephroprotective effect of pioglitazone would be in line with the results of previous studies on PPAR-gamma agonists in animal models of renal failure[52] and diabetic nephropathy,[53,54] the data of this study do not suffice to confirm this hypothesis, so that further experiments designed to address the nephroprotective impact of pioglitazone are required.

CONCLUSIONS

The current study is the first systematic in vivo examination on the impact of pioglitazone on the degeneration of cryopreserved valved aortic grafts. Systemic PPAR-gamma activation prevents inflammatory processes as well as intima and media calcification in aortic valve conduits and seems to inhibit functional impairment of the implanted aortic valve. To further elucidate the potential therapeutic role of PPAR-gamma regulation for an improvement of biological graft durability, particularly analyzing effects on inflammation, calcifying degeneration, and intima hyperplasia, translational studies and long-term follow-up data should be striven for.

ACKNOWLEDGMENTS

The authors gratefully thank Gisela Müller (Department of Cardiac Surgery and Research Group for Experimental Surgery, Medical Faculty, Heinrich Heine University Duesseldorf, Germany) for her help in the PCR experiments as well as the Institute of Clinical Chemistry and Laboratory Diagnostics, Heinrich Heine University, Medical Faculty, Duesseldorf, Germany) for the blood analyses. The generous support of the S. Bunnenberg Foundation to the Cardiovascular Research Facilities at Heinrich-Heine-University is greatly appreciated.

REFERENCES

1. Stassano P, Di Tommaso L, Monaco M, et al. Aortic valve replacement: a prospective randomized evaluation of mechanical versus biological valves in patients ages 55 to 70 years. *J Am Coll Cardiol.* 2009;54: 1862–1868.
2. Chiang YP, Chikwe J, Moskowitz AJ, et al. Survival and long-term outcomes following bioprosthetic vs mechanical aortic valve replacement in patients aged 50 to 69 years. *JAMA*. 2014;312:1323–1329.
3. Mohty D, Pibarot P, Côté N, et al. Hypoadiponectinemia is associated with valvular inflammation and faster disease progression in patients with aortic stenosis. *Cardiology*. 2011;118:140–146.
4. Meyer SR, Nagendran J, Desai LS, et al. Decellularization reduces the immune response to aortic valve allografts in the rat. *J Thorac Cardiovasc Surg.* 2005;130:469–476.
5. Lehr EJ, Rayat GR, Chiu B, et al. Decellularization reduces immunogenicity of sheep pulmonary artery vascular patches. *J Thorac Cardiovasc Surg.* 2011;141:1056–1062.
6. Welters MJ, Oei FB, Vaessen LM, et al. Increased numbers of circulating donor-specific T helper lymphocytes after human heart valve transplantation. *Clin Exp Immunol.* 2001;124:353–358.
7. Vogt PR, Stallmach T, Niederhäuser U, et al. Explanted cryopreserved allografts: a morphological and immunohistochemical comparison between arterial allografts and allograft heart valves from infants and adults. *Eur J Cardiothorac Surg.* 1999;15:639–645. discussion 44-5.
8. Kanter KR, Kirshbom PM, Kogon BE. Redo aortic valve replacement in children. *Ann Thorac Surg.* 2006;82:1594–1597.
9. Kowert A, Vogt F, Beiras-Fernandez A, et al. Outcome after homograft redo operation in aortic position. *Eur J Cardiothorac Surg.* 2012;41:404–408.
10. Jiang C, Ting AT, Seed B. PPAR-gamma agonists inhibit production of monocyte inflammatory cytokines. *Nature.* 1998;391:82–86.
11. Ricote M, Li AC, Willson TM, et al. The peroxisome proliferator-activated receptor-gamma is a negative regulator of macrophage activation. *Nature*. 1998;391:79–82.
12. Marx N, Kehrle B, Kohlhammer K, et al. PPAR activators as antiinflammatory mediators in human T lymphocytes: implications for atherosclerosis and transplantation-associated arteriosclerosis. *Circ Res.* 2002;90: 703–710.
13. Li F, Cai Z, Chen F, et al. Pioglitazone attenuates progression of aortic valve calcification via down-regulating receptor for advanced glycation end products. *Basic Res Cardiol.* 2012;107:306.
14. Teshima EBF, Aubin H, Assmann A, et al. PPAR-gamma activation for inhibition of in vivo calcific degeneration of cardiovascular bioprostheses. Heart Valve Society 1st Annual Meeting, Monte Carlo, Monaco, 2015.
15. Assmann A, Akhyari P, Delfs C, et al. Development of a growing rat model for the in vivo assessment of engineered aortic conduits. *J Surg Res.* 2012;176:367–375.
16. Assmann A, Delfs C, Munakata H, et al. Acceleration of autologous in vivo recellularization of decellularized aortic conduits by fibronectin surface coating. *Biomaterials*. 2013;34:6015–6026.
17. Assmann A, Horstkötter K, Munakata H, et al. Simvastatin does not diminish the in vivo degeneration of decellularized aortic conduits. *J Cardiovasc Pharmacol.* 2014;64:332–342.
18. Assmann A, Zwirnmann K, Heidelberg F, et al. The degeneration of biological cardiovascular prostheses under pro-calcific metabolic conditions in a small animal model. *Biomaterials*. 2014;35:7416–7428.
19. Wang K, Zhou Z, Zhang M, et al. Peroxisome proliferator-activated receptor gamma down-regulates receptor for advanced glycation end products and inhibits smooth muscle cell proliferation in a diabetic and nondiabetic rat carotid artery injury model. *J Pharmacol Exp Ther.* 2006; 317:37–43.
20. Dobrian AD, Schriver SD, Khraibi AA, et al. Pioglitazone prevents hypertension and reduces oxidative stress in diet-induced obesity. *Hypertension*. 2004;43:48–56.
21. Zanchi A, Dulloo AG, Perregaux C, et al. Telmisartan prevents the glitazone-induced weight gain without interfering with its insulin-sensitizing properties. *Am J Physiol Endocrinol Metab.* 2007;293:E91–E95.
22. Blalock EM, Phelps JT, Pancani T, et al. Effects of long-term pioglitazone treatment on peripheral and central markers of aging. *PLoS One*. 2010;5:e10405.
23. Munakata H, Assmann A, Poudel-Bochmann B, et al. Aortic conduit valve model with controlled moderate aortic regurgitation in rats: a technical modification to improve short- and long-term outcome and to increase the functional results. *Circ J.* 2013;77:2295–2302.
24. Sun H, Lu X, Wu S, et al. The effects of C-reactive protein, interleukin-6, and tumor necrosis factor-alpha in rat allograft adventitial inflammation and allograft arteriosclerosis. *Transpl Proc*. 2009;41:3909–3912.
25. Okada M, Yan SF, Pinsky DJ. Peroxisome proliferator-activated receptor-gamma (PPAR-gamma) activation suppresses ischemic induction of Egr-1 and its inflammatory gene targets. *FASEB J.* 2002;16:1861–1868.
26. Ross R. Atherosclerosis–an inflammatory disease. *N Engl J Med.* 1999; 340:115–126.
27. Rosenfeld ME, Ross R. Macrophage and smooth muscle cell proliferation in atherosclerotic lesions of WHHL and comparably hypercholesterolemic fat-fed rabbits. *Arteriosclerosis*. 1990;10:680–687.
28. Spagnoli LG, Orlandi A, Santeusanio G. Foam cells of the rabbit atherosclerotic plaque arrested in metaphase by colchicine show a macrophage phenotype. *Atherosclerosis*. 1991;88:87–92.
29. Lamharzi N, Renard CB, Kramer F, et al. Hyperlipidemia in concert with hyperglycemia stimulates the proliferation of macrophages in atherosclerotic lesions: potential role of glucose-oxidized LDL. *Diabetes*. 2004;53: 3217–3225.
30. Yunna C, Mengru H, Lei W, et al. Macrophage M1/M2 polarization. *Eur J Pharmacol.* 2020;877:173090.
31. Wang LX, Zhang SX, Wu HJ, et al. M2b macrophage polarization and its roles in diseases. *J Leukoc Biol.* 2019;106:345–358.
32. Shapouri-Moghaddam A, Mohammadian S, Vazini H, et al. Macrophage plasticity, polarization, and function in health and disease. *J Cel Physiol*. 2018;233:6425–6440.
33. Foryst-Ludwig A, Hartge M, Clemenz M, et al. PPARgamma activation attenuates T-lymphocyte-dependent inflammation of adipose tissue and development of insulin resistance in obese mice. *Cardiovasc Diabetol.* 2010;9:64.
34. Kintscher U, Hartge M, Hess K, et al. T-lymphocyte infiltration in visceral adipose tissue: a primary event in adipose tissue inflammation and the development of obesity-mediated insulin resistance. *Arterioscler Thromb Vasc Biol.* 2008;28:1304–1310.
35. Murakami-Nishida S, Matsumura T, Senokuchi T, et al. Pioglitazone suppresses macrophage proliferation in apolipoprotein-E deficient mice by activating PPARgamma. *Atherosclerosis*. 2019;286:30–39.
36. Zhang Y, Yang X, Bian F, et al. TNF-alpha promotes early atherosclerosis by increasing transcytosis of LDL across endothelial cells: crosstalk between NF-kappaB and PPAR-gamma. *J Mol Cel Cardiol*. 2014;72:85–94.
37. Wei Q, Ren X, Jiang Y, et al. Advanced glycation end products accelerate rat vascular calcification through RAGE/oxidative stress. *BMC Cardiovasc Disord.* 2013;13:13.
38. Ihm SH, Chang K, Kim HY, et al. Peroxisome proliferator-activated receptor-gamma activation attenuates cardiac fibrosis in type 2 diabetic rats: the effect of rosiglitazone on myocardial expression of receptor for advanced glycation end products and of connective tissue growth factor. *Basic Res Cardiol.* 2010;105:399–407.
39. Wang L, Chen K, Liu K, et al. DHA inhibited AGEs-induced retinal microglia activation via suppression of the PPARgamma/NFkappaB pathway and reduction of signal transducers in the AGEs/RAGE axis recruitment into lipid rafts. *Neurochem Res.* 2015;40:713–722.
40. Katz R, Budoff MJ, Takasu J, et al. Relationship of metabolic syndrome with incident aortic valve calcium and aortic valve calcium progression: the Multi-Ethnic Study of Atherosclerosis (MESA). *Diabetes*. 2009;58: 813–819.
41. Kaden JJ, Bickelhaupt S, Grobholz R, et al. Expression of bone sialoprotein and bone morphogenetic protein-2 in calcific aortic stenosis. *J Heart Valve Dis.* 2004;13:560–566.
42. Prince M, Banerjee C, Javed A, et al. Expression and regulation of Runx2/Cbfa1 and osteoblast phenotypic markers during the growth and differentiation of human osteoblasts. *J Cel Biochem*. 2001;80:424–440.
43. Li AC, Brown KK, Silvestre MJ, et al. Peroxisome proliferator-activated receptor gamma ligands inhibit development of atheroscle-

rosis in LDL receptor-deficient mice. *J Clin Invest.* 2000;106:523–531.
44. Chen Z, Ishibashi S, Perrey S, et al. Troglitazone inhibits atherosclerosis in apolipoprotein E-knockout mice: pleiotropic effects on CD36 expression and HDL. *Arterioscler Thromb Vasc Biol.* 2001;21:372–377.
45. Otto CM, Kuusisto J, Reichenbach DD, et al. Characterization of the early lesion of 'degenerative' valvular aortic stenosis. Histological and immunohistochemical studies. *Circulation*. 1994;90:844–853.
46. Lin TH, Yang RS, Tang CH, et al. PPARgamma inhibits osteogenesis via the down-regulation of the expression of COX-2 and iNOS in rats. *Bone*. 2007;41:562–574.
47. Pelham CJ, Keen HL, Lentz SR, et al. Dominant negative PPARgamma promotes atherosclerosis, vascular dysfunction, and hypertension through distinct effects in endothelium and vascular muscle. *Am J Physiol Regul Integr Comp Physiol.* 2013;304:R690–R701.
48. Halabi CM, Beyer AM, de Lange WJ, et al. Interference with PPAR gamma function in smooth muscle causes vascular dysfunction and hypertension. *Cell Metab*. 2008;7:215–226.
49. Xiang AH, Peters RK, Kjos SL, et al. Effect of thiazolidinedione treatment on progression of subclinical atherosclerosis in premenopausal women at high risk for type 2 diabetes. *J Clin Endocrinol Metab.* 2005;90:1986–1991.
50. Mazzone T, Meyer PM, Feinstein SB, et al. Effect of pioglitazone compared with glimepiride on carotid intima-media thickness in type 2 diabetes: a randomized trial. *JAMA*. 2006;296:2572–2581.
51. Minamikawa J, Tanaka S, Yamauchi M, et al. Potent inhibitory effect of troglitazone on carotid arterial wall thickness in type 2 diabetes. *J Clin Endocrinol Metab.* 1998;83:1818–1820.
52. Newaz M, Yousefipour Z, Oyekan A. Role of PPAR-gamma on the pathogenesis and vascular changes in glycerol-induced acute renal failure. *Pharmacol Res.* 2006;54:234–240.
53. Toblli JE, Ferrini MG, Cao G, et al. Antifibrotic effects of pioglitazone on the kidney in a rat model of type 2 diabetes mellitus. *Nephrol Dial Transpl.* 2009;24:2384–2391.
54. Okada T, Wada J, Hida K, et al. Thiazolidinediones ameliorate diabetic nephropathy via cell cycle-dependent mechanisms. *Diabetes*. 2006;55:1666–1677.